Journal of Power Sources 343 (2017) 183–187

Contents lists available at ScienceDirect

Journal of Power Sources

journal homepage: www.elsevier.com/locate/jpowsour

Estimating the state of charge of MH-Ni batteries by measuring their stable internal pressure

Jian Zhang [a], Guangjie Shao [b], Weiwen Guo [a, b], Yuwan Lou [a, *], Baojia Xia [a]

[a] Shanghai Institute of Microsystem and Information Technology, Chinese Academy of Sciences, Shanghai, 200050, China
[b] College of Environmental and Chemical Engineering, Yanshan University, Qinhuangdao, Hebei, 066004, China

HIGHLIGHTS

- MH-Ni batteries were built with internal pressure sensors.
- SOC and the stable internal pressure have a one-to-one correspondence.
- The correlation mechanism between internal pressure and SOC was discussed.

ARTICLE INFO

Article history:
Received 19 October 2016
Received in revised form
17 December 2016
Accepted 6 January 2017

Keywords:
MH-Ni battery
Hybrid electric vehicle
Stable internal pressure
State of charge
Estimate

ABSTRACT

Nickel metal hydride (MH-Ni) batteries are widely used in hybrid electric vehicles (HEVs). Estimating a battery's state of charge (SOC) remains challenging in practical applications, and it is also the core technology. Because MH-Ni batteries exhibit high rates of self-discharge and have flat and broad charge-discharge voltage plateaus, the estimation of their SOC through their voltage, current, internal resistance, and temperature is not accurate and has a large cumulative error. In this study, a new method for estimating SOC based on battery's stable internal pressure is proposed using the one-to-one correspondence between the hydrogen equilibrium pressure and the reversible hydrogen-storage capacity described by the pressure–concentration–isotherm (P-C-T) curves of hydrogen storage alloys. The actual SOC and the stable internal pressure of the battery have a one-to-one correspondence after the battery was stored at different temperatures and SOCs, and this relationship is maintained after different cycling number and after four years of storage.

1. Introduction

Because of their high charge-discharge power densities, high safety, and good performances at low temperatures, MH-Ni batteries are widely used for hybrid electric vehicles (HEVs) [1–3]. Unlike electric cars, which typically operate initially from a fully charged state during use and occasionally reach a fully discharged state allowing corrections to state of charge (SOC) estimations, HEVs batteries are often operated at a SOC of ~50% throughout their life. Typical SOC for HEVs batteries range from 30% to 80%. If the battery does not work in this SOC range, the battery life will be shortened, and its effective energy storage and energy efficiency will also be reduced [4]. Accordingly, new methods of SOC estimation are in urgent demand for HEV batteries.

In HEVs, battery management system (BMS) must rapidly and accurately inform vehicle control systems of the battery's SOC to determine whether it can input or output sufficient energy. This allows the vehicle's engine to maintain an optimal working condition and reduce energy consumption and vehicle emissions. The accuracy of SOC estimation needs to be improved to improve the reliability of BMS [5].

Existing methods such as the integration of ampere hours [6–8], measurement of internal resistance [9], measurement of open-circuit (load) voltage [10–12], use of artificial intelligence [13–15], and Kalman filtering [16–18] often suffer from low accuracies and large accumulated errors. The ampere-hour integration method is the most commonly used method in commercial electric vehicles. Because of the limitation of sampling precision of current sensor, less than 100% coulombic efficiency and self-discharge

* Corresponding author: Research Center for New Energy Technology, Shanghai Institute of Microsystem and Information Technology, Chinese Academy of Sciences, Shanghai, 200050, China.
E-mail address: zjskycn@mail.sim.ac.cn (Y. Lou).

http://dx.doi.org/10.1016/j.jpowsour.2017.01.031
0378-7753/

current is not through the external circuit, charge-discharge capacity calculations do not accurately reflect a battery's actual SOC. After considerable use of a battery, the accumulated error in the estimated SOC increases, especially for MH-Ni batteries. Unlike that of a Li-ion battery, a MH-Ni battery's open-circuit and charge-discharge voltages are very stable over a wide range of temperatures and SOCs. Therefore, even a small voltage change can indicate a large change in the SOC. Since HEVs batteries operate under these conditions, common voltage-based methods cannot be used to accurately estimate SOC. SOC estimated by internal resistance method is measured by galvanostatic discharge at a certain temperature. During charging and discharging, MH-Ni battery's SOC is not a monotonic function of its internal resistance, and therefore, a battery's internal resistance is rarely used to measure the SOC in HEVs.

In this study, we characterize a MH-Ni battery through the measurement of internal pressure after internal gas stabilization and propose a new method for SOC estimation based on these measurements.

2. Experimental

2.1. Material and methods

The internal pressure of a sealed battery can be measured either indirectly or directly. The indirect method measures internal pressure through measurements of resistance strain or mechanical strain, which do not harm the battery but have low precision and are impacted by vibrations, dust, and other environmental factors. In this work, internal battery pressure was measured directly by building a Nanjing Wotian PC9 type pressure sensor inside a battery. Stainless steel (316L), which is alkali resistant, was used in the sensor package. Measurements were made from 0 psi to 145 psi with a precision of 0.1 psi and a high stability. The working temperature of the sensor was from −40°C to 100 °C.

The pressure sensor acted as the battery cap, and was welded to the cathode collector of the MH-Ni battery (QNY6 type D, Shanghai Wanhong Power Energy Co.). The battery was then mechanically sealed to prevent leakage. The sensor's top cover was positioned to allow adequate space for battery combination, and the same battery size was retained, allowing it to be combined with other batteries in a real vehicle battery system, as shown in Fig. 1.

2.2. Characterization

The battery was maintained at a constant temperature in a thermostat oven. Arbin MIT2000 (American Arbin Co.) and 5 V/50 A Neware (Shenzhen Neware Co.) battery testing instruments were used to charge the battery at 1C rate for 72 min (controlled by $-\triangle V = 10$ mV). The battery was discharged to 1.0 V at a rate of 1 C. The battery's internal pressure and SOC were measured after the battery was stored at different temperatures and SOCs. The battery's internal pressure and SOC were also measured after different cycling number.

The battery was cycled under simulated conditions at 25 ± 2 °C. The simulated conditions were adapted from Ref. [19], each cycle is equivalent to 1000 simulated HEV charge-discharge cycles. The battery was stored at 25 °C at 50% SOC for four years. The battery was activated once every three months at 0.2 C and then discharged to 50% SOC such that the open-circuit voltage was above 1.2 V throughout the storage process.

3. Results and discussion

To evaluate the stability of a battery's internal pressure, the same battery was charged to different SOCs at 1 C and stored at 25 °C. The battery's internal pressure and the rate at which the pressure changed over time are shown in Fig. 2. Fig. 2(a) shows the internal pressure over the full SOC range from 0% to 100%. After a prolonged storage time, the battery's internal pressure decreased and reached a stable value after 5 h. Fig. 2(b) shows that the internal pressure changed at a rate of less than 6.2×10^{-4} psi/s after 5 h, indicating that the pressure was stable. According to the P-C-T curves, a stable equilibrium partial pressure of hydrogen was achieved in the battery along with a small amount of air (O_2 and N_2) that was introduced during battery production. During the late stages of charging, O_2 and H_2 were evolved at the cathode and the anode, respectively, as shown in Reaction (1). A higher SOC corresponded to the release of more gaseous product and a higher internal battery pressure. As shown in Fig. 2(a), the battery reached its highest internal pressure at a SOC of 100%, while that with a SOC of 90% had the second highest internal pressure. O_2 diffused from the cathode, passed through the separator, and reached the surface of the anode. At this point, it reacted quickly with H to form H_2O via Reactions (2) or (3) [20]. After a long resting time, all the O_2 in the battery was consumed. As a result, the internal pressure increased along with the rate of pressure change (Fig. 2 (b)). This increased the time before stability was reached. The rate at which the pressure changed was the greatest at SOC of 100%, and it was next highest at SOC of 90%.

$$\text{Cathode}: \quad 4OH^- \rightarrow 2H_2O + O_2 + 4e^- \quad (1)$$

$$\text{Anode}: \quad O_2 + 2H_2O + 4e^- \rightarrow 4OH^- \quad (2)$$

$$\text{or} \quad 4MH + O_2 \rightarrow 4M + 2H_2O \quad (3)$$

Gaseous hydrogen also maintains an equilibrium with atomic hydrogen in the hydrogen-storage alloy. Therefore, the internal pressure is the sum of the partial pressure and the pressure of the

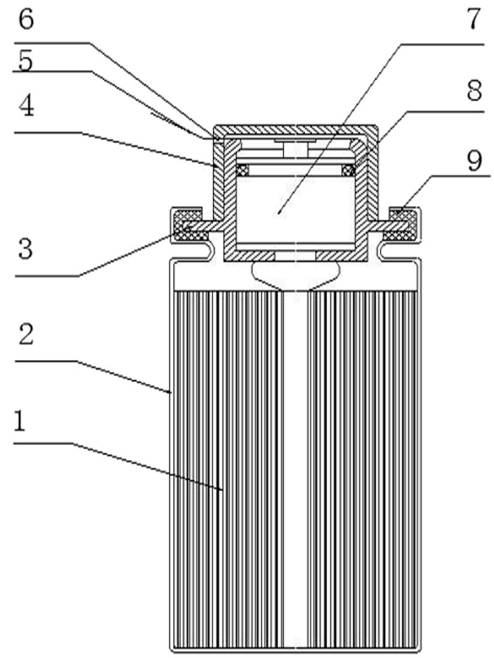

Fig. 1. Diagram of a MH-Ni cell with built-in pressure sensor. 1: electrode group, 2: steel shell (negative electrode), 3: fixed bottom cover for pressure sensor, 4: fixed top cover for pressure sensor, 5: pressure sensor wire, 6: pressure sensor wire hole, 7: pressure sensor, 8: O-ring, 9: battery sealing.

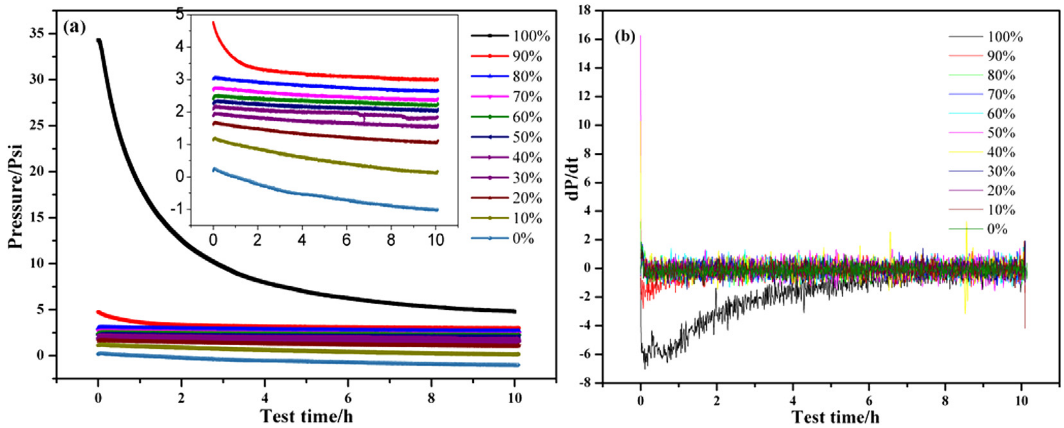

Fig. 2. Battery's internal pressure (a) and the rate of pressure change (b) *vs*. time under rest at different SOCs.

inert gas sealed inside the battery during manufacturing.

Clearly, higher internal pressures indicate a higher partial pressure of hydrogen gas, an increased amount of hydrogen stored in the alloy, and a higher SOC of the battery. In this study, final stable pressures were the same when the batteries were either charged or discharged to reach a desired SOC, suggesting that the internal pressure of a MH-Ni battery has a one-to-one relationship with the battery's SOC at a constant temperature.

The battery was charged to a SOC of 90% at 1 C at different temperatures, and the resulting relationship between internal pressure and time is shown in Fig. 3. The battery's internal pressure was stable within 10 h at the different temperatures. Higher temperatures resulted in higher internal pressures, which is in agreement with the ideal gas law. Relationships between the internal pressure and SOC of different batteries at 25 °C and the same battery at different temperatures are shown in Fig. 4(a) and (b), respectively. The different batteries exhibited different pressures even at the same SOC and temperature. These differences resulted from small variations in cell preparation. Therefore, this method gives more precise results if calibrated for each battery individually. For the same battery at a SOC between 30% and 80%, the stable internal pressure displayed approximately linear relationship with its SOC, allowing the accurate determination of SOC.

The relationship between internal pressure and SOC before, after 16 and 32 simulation test cycles is shown in Fig. 5. The charge and discharge curves before and after simulation test cycles are shown in Fig. 6.

As shown in Fig. 5, the battery's internal pressure and SOC retained an approximate linear relation after 16 and 32 simulation test cycles at a SOC between 30% and 80%, but the slope of the curve clearly increased after cycling. Even at a constant temperature and SOC, the internal pressure of the battery increased, indicating that the battery's hydrogen partial pressure increased. This increase in pressure was caused by the corrosion of the AB_5 hydrogen-storage alloy in the strong alkaline electrolyte during cycling [21,22], as shown in Reaction (4). This corrosion decreased the amount of anode's hydrogen-storage alloys, resulted in the remaining hydrogen-storage alloys being forced to store more hydrogen per unit mass, and the hydrogen partial pressure increased. However, conjugation reactions (Reactions (5)) during alloy corrosion released gaseous hydrogen, causing the hydrogen partial pressure to increase. The increase of gaseous hydrogen in sealed battery will make the content of H in hydrogen-storage alloy higher and stable internal pressure increase at equilibrium under the same conditions, causing the slope of stable internal pressure-SOC curve to increases. During MH-Ni battery design, the capacity of anode is often excessive relative to cathode [23,24], that is, the capacity limitation electrode is the cathode, so the SOC does not change.

Therefore, it was necessary to correct the measurement based on the battery's actual condition when the SOC was estimated from internal pressure.

$$M \rightarrow M^{+} + xe^{-} \tag{4}$$

$$xH_2O + xe^{-} \rightarrow xOH^{-} + \frac{x}{2}H_2 \tag{5}$$

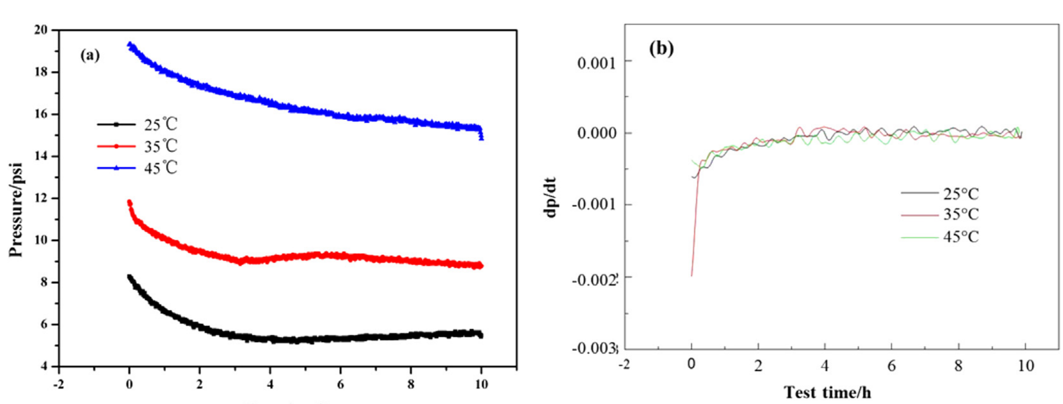

Fig. 3. Battery's internal pressure (a) and the rate of pressure change (b) *vs*. time at SOC of 90%.

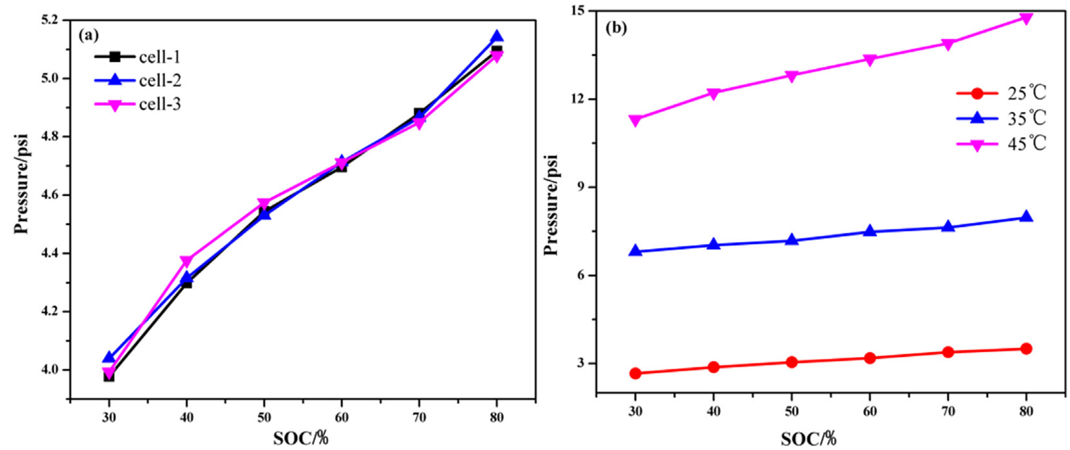

Fig. 4. Relationships between the internal pressure and SOC for (a) different batteries at 25 °C and for (b) the same battery at different temperatures.

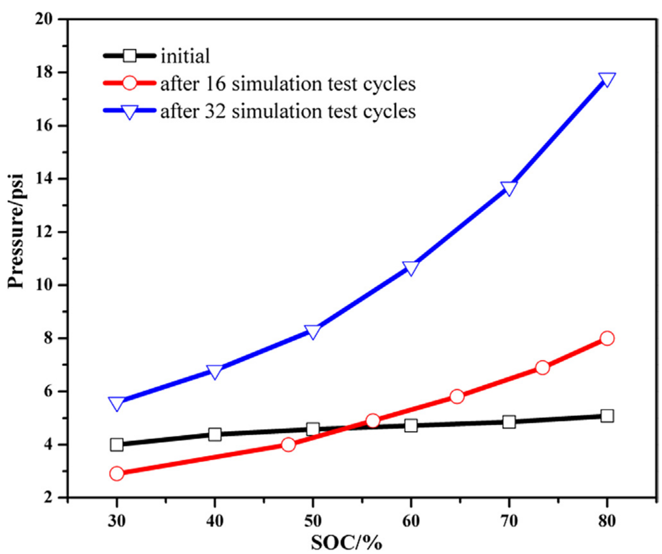

Fig. 5. Relationship between internal pressure and SOC before and after simulation test cycling at 25 °C.

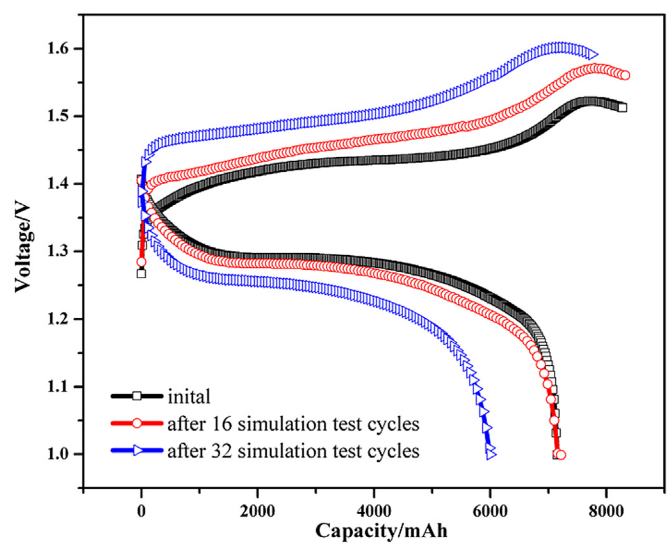

Fig. 6. Charge-discharge curves at 1C of the battery before and after simulation test cycling at 25 °C.

Fig. 6 shows that the battery's capacity and charging-discharging characteristics are almost the same before and after 16 simulation test cycling. After 16 simulation test cycling, polarization slightly increased during the late stages of charging and discharging. The DC resistance of the battery was 4.84 mΩ, a 25.7% increase compared to that before cycling. This increase was caused by the corrosion of the hydrogen-storage alloy. After 32 simulation test cycling, discharging capacity is reduced to 84.05% of the initial capacity and polarization clearly increased during the charging and discharging, as shown in Fig. 6. The DC resistance of the battery significantly increased to 11.36 mΩ, indicating hydrogen-storage alloy suffered serious corrosion, discharging capacity of the battery decreased significantly. To account for the fact that batteries are stored for a long time during actual use, we stored batteries at 25 °C for four years, before measuring their internal pressures at different temperatures to estimate their SOC, as shown in Fig. 7. Clearly, the internal pressure and the SOC of the battery still had a one-to-one relationship.

Overall, the available discharge capacity of the hydrogen-storage alloy anode and the battery's SOC were related. When a battery was charged or discharged to the same capacity, changes in

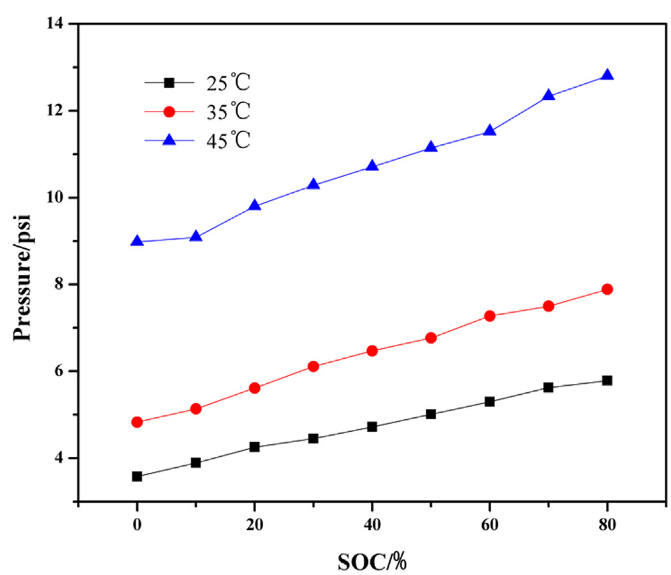

Fig. 7. Relationship between internal pressure and SOC of a battery stored for four years at 25 °C.

the anode's capacity inevitably led to changes in the partial pressure of hydrogen in the hydrogen-storage alloy. At a constant temperature, the internal pressure and the actual SOC displayed a one-to-one relationship.

4. Conclusions

MH-Ni batteries (type D) were built with embedded internal pressure sensors. The relationship between the internal pressure of the battery was studied over time at different SOCs at 25 °C and at constant SOC at different temperatures. The battery's internal pressure became stable over time. After 16 and 32 simulation test cycles under HEVs-like working conditions and after four years of storage at room temperature, the battery's internal pressure retained a one-to-one relationship with the its SOC. This is a new method for estimating the SOCs of MH-Ni batteries.

Acknowledgements

This work was supported by National Science Foundation of China (No. 51277173).

References

[1] W.H.H. Zhu, Y. Zhu, B.J. Tatarchuk, Int. J. Hydrogen Energy 39 (2014) 19789–19798.
[2] W.H.H. Zhu, Y. Zhu, Z. Davis, B.J. Tatarchuk, Appl. Energy 106 (2013) 307–313.
[3] J.Q. Kang, F.W. Yan, P. Zhang, C.Q. Du, Energy 70 (2014) 618–625.
[4] Y.H. Zhang, W.J. Song, S.L. Lin, J. Lv, Z.P. Feng, J. Renew. Sustain. Energy 5 (021403) (2013) 1–10.
[5] B. Xia, C. Mi, J. Power Sources 308 (2016) 83–96.
[6] Z.W. Deng, L. Yang, Y.S. Cai, H. Deng, L. Sun, Energy 112 (2016) 469–480.
[7] H.F. Yu, R.G. Lu, C.N. Zhu, R. Ma, Trans. China Electrotech. Soc. 27 (2012) 12–18.
[8] M. García-Plaza, D. Serrano-Jimenez, J. Eloy-García Carrasco, J. Alonso-Martínez, J. Power Sources 275 (2015) 595–604.
[9] Y.H. Chiang, W.Y. Sean, J.C. Ke, J. Power Sources 196 (2011) 3921–3932.
[10] F.D. Zheng, Y.J. Xing, J.C. Jiang, B.X. Sun, J.H. Kim, M. Pecht, Appl. Energy 183 (2016) 513–525.
[11] L.T. Zhu, Z.C. Sun, H.F. Dai, X.Z. Wei, Appl. Energy 155 (2015) 91–109.
[12] C.H. Weng, J. Sun, H. Peng, J. Power Sources 258 (2014) 228–237.
[13] Y.Q. Shen, Energy Convers. Manage. 51 (2010) 1093–1098.
[14] B. Chen, Y.L. Zhou, J.X. Zhang, J.P. Wang, B.G. Cao, Energy Convers. Manage. 50 (2009) 3078–3086.
[15] S.J. Tong, J.H. Lacap, J.W. Park, J. Energy Storage 7 (2016) 236–243.
[16] L. Xu, J.P. Wang, Q.S. Chen, Energy Convers. Manage. 53 (2012) 33–39.
[17] J.P. Wang, J.H. Guo, L. Ding, Energy Convers. Manage. 50 (2009) 3182–3186.
[18] R.H. Milocco, B.E. Castro, J. Power Sources 194 (2009) 558–567.
[19] Measurement Method of High Power Nickel Metal Hydride Battery 2008 Annual, Office of the Ministry of Science and Technology 863 Modern Transportation Technology, Beijing, 2008.
[20] D.J. Cuscueta, H.R. Salva, A.A. Ghilarducci, J. Power Sources 196 (2011) 4067–4071.
[21] P. Leblanc, C. Jordy, B. Knosp, P. Blanchard, J. Electrochem. Soc. 145 (1998) 860–863.
[22] C.S. Wang, M. Marrero-Cruz, M.P. Soriaga, D. Serafini, S. Srinivasan, Electrochim. Acta 47 (2002) 1069–1078.
[23] B.J. Xia, G.P. Yin, X.Q. Cheng, J.L. Li, Battery Bimon. 30 (2000) 59–61.
[24] Z.R. Chang, G. En-bo Shang, D. Cheng, Y.J. Xu, Battery Bimon. 37 (2007) 367–369.